Analytical Solution of Joule-Heating Equation for Metallic Single-Walled Carbon Nanotube Interconnects

Rekha Verma, Sitangshu Bhattacharya, and Santanu Mahapatra, *Senior Member, IEEE*

***Abstract*—In this paper, we address a closed-form analytical solution of the Joule-heating equation for metallic single-walled carbon nanotubes (SWCNTs). Temperature-dependent thermal conductivity κ has been considered on the basis of second-order three-phonon Umklapp, mass difference, and boundary scattering phenomena. It is found that κ, in case of pure SWCNT, leads to a low rising in the temperature profile along the via length. However, in an impure SWCNT, κ reduces due to the presence of mass difference scattering, which significantly elevates the temperature. With an increase in impurity, there is a significant shift of the hot spot location toward the higher temperature end point contact. Our analytical model, as presented in this study, agrees well with the numerical solution and can be treated as a method for obtaining an accurate analysis of the temperature profile along the CNT-based interconnects.**

***Index Terms*—Carbon nanotubes, interconnects, Joule heating, thermal conductivity.**

I. Introduction

THERMAL management in aggressively scaled low-dimensional devices is gaining momentum and is one of the key factors in the understanding of proper electrothermal analyses in modern state-of-the-art multilevel chip design. Metallic single-walled carbon nanotubes (SWCNTs) have been found to possess very high lattice thermal conductivity κ [1]–[3], which makes them good candidates for potential thermal materials over copper interconnects [4], [5]. Recently, there have been few investigations that predict the electrical and thermal characteristics of metallic SWCNT as interconnects [5]–[9]. These studies are however based on the assumption of either constant thermal conductivity over a wide range of temperatures or possession of empirical dependence, together with negligence of mass-difference scattering, which must be taken into account to model the commonly encountered situation where the difference in the atomic mass of carbon atoms are introduced unintentionally at the ends of the CNT under the prevailing fabrication methods [10]. This introduction of carbon isotopes in pure SWCNT makes it an impure one and marks wide variations in phonon-assisted thermal conductivity. Unlike aluminum and copper, the thermal conductivity of SWCNT exhibits an extremely nonlinear behavior over the temperature zone of interest in interconnects [2]. This is due to the presence of second-order three-phonon Umklapp, mass difference, and boundary-scattering phenomena, which characterize $1/T^2$ behavior beyond room temperature [1], [2]. This nonlinearity in the thermal conductivity results in an involved mathematical formulation of the solution of the Joule-heating equation [11], [12].

Techniques for the solution of the Joule-heating equation, when the thermal conductivity is a function of temperature, [11], [13] are available; however, due to the presence of singularity [13] resulting from the available empirically derived temperature-dependent κ for metallic SWCNT [1], a proper solution is still unknown. Moreover, there are a few reports that represent the numerical analysis of the Joule-heating equation by considering a temperature-dependent thermal conductivity of SWCNTs [9]. Although the solution to these numerical models are important, an analytical method is also needed to exhibit and explain the physical interactions among various scattering phenomena, heat conduction, convection, and radiation, particularly in the case of bundles of SWCNT as the state-of-the-art vias surrounded by a dielectric. Since the difficulties in fabrication of horizontally aligned local, intermediate, and global interconnects using bundles of metallic SWCNTs are one of the bottleneck issues in recent interconnect technology, ease in the incorporation of their vertical bundles as vias demands that an analytical Joule-heating conduction mechanism in a single metallic SWCNT be the first step in the investigation of accurate electrothermal study of the bundles.

In this paper, we address a closed-form solution of the Joule-heating equation for metallic SWCNT using temperature-dependent κ on the basis of the Umklapp, mass difference, and boundary scattering phenomena. We use Kirchoff's transformation to linearize the relation between the fictitious and actual temperatures [13]. With this, we demonstrate that the temperature profile along the length of the SWCNT strongly depends on not only the length but also the form factor of the mass difference scattering. Additionally, we show that the temperature rise in an impure SWCNT suffers wide deviation from that of the pure at different current levels. Our analytical model agrees well with the numerical solution as presented

Manuscript received May 4, 2011; revised July 7, 2011; accepted July 22, 2011. Date of publication September 12, 2011; date of current version October 21, 2011. This work was supported by the Department of Science and Technology, India, under Grant SR/FTP/ETA-37/08. The review of this paper was arranged by Editor R. Venkatasubramanian.

The authors are with the Nano-Scale Device Research Laboratory, Centre for Electronics Design and Technology, Indian Institute of Science, Bangalore 560012, India (e-mail: rekha.verma26@gmail.com; isbsin@yahoo.co.in; santanu@cedt.iisc.ernet.in).

Color versions of one or more of the figures in this paper are available online at http://ieeexplore.ieee.org.

Digital Object Identifier 10.1109/TED.2011.2163516

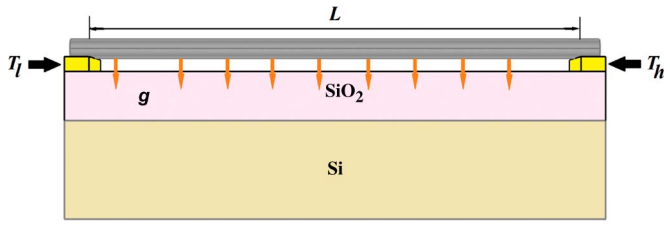

Fig. 1. Schematic representation of a suspended SWCNT of length L (adapted after [9] and [12]), the two ends of which are fixed to the metallic contacts with contact resistance R_c, at different temperatures T_l and T_h. The downward arrows represent the net heat loss per unit length to the substrate SiO_2, which is essentially the heat transfer coefficient g.

here and can be put forth to carry out an accurate analysis of temperature profile in the CNT-based interconnects.

II. Model Development

We start with the expression of the steady-state Joule-heating equation with a temperature-dependent thermal conductivity along the length of the SWCNT [1], [11]

$$A\nabla(\kappa\nabla T) + p - g(T - T') = 0 \tag{1}$$

where $A = \pi db$ is the cross-sectional area; d and b are the diameter and the tube wall thickness of the SWCNT, respectively; $T' = 1/2(T_h + T_l)$, T_h, and T_l are the temperatures at two contacts, i.e., the driving force for transport $p = j^2(\rho(T) - \rho_c)A$; j is the current density in amperes per square meter through the SWCNT; $\rho(T)$ and ρ_c are the total electrical resistivity of the nanotube and contacts, respectively; L (in Fig. 1) is the tube length; and g is the net heat loss to the substrate per unit length, which is essentially the heat transfer coefficient. Fig. 1 represents the schematic diagram of a suspended SWCNT for the present case. It should be noted that (1) is also known as the fin equation [14], except for the additional term g. It is well known that the diffusive electrical resistance of a metallic SWCNT strongly depends on temperature, occurring due to the longitudinal acoustic, longitudinal optical, and zone boundary phonon-scattering phenomena [15]. However, in this case, we have neglected these dependencies since, within a 2-μm via length, the resistance is a weak function of temperature between 300 and 500 K [12].

In case of temperature-independent thermal conductivity, using the boundary condition $T(-L/2) = T(L/2) = T_0$, the solution to (1) can be written as

$$T(x) = T_0 + \frac{p}{g}\left[1 - \frac{\cosh(x/L_H)}{\cosh(L/2L_H)}\right] \tag{2}$$

where $L_H = \sqrt{A\kappa/g}$ is the characteristic thermal heating length along the SWCNT length and $-L/2 < x < L/2$.

For temperature-dependent thermal conductivity, the solution of (1) can be formulated by assuming a fictitious temperature $\theta(x)$ at each point x connected by the actual temperature T through the steady-state Kirchoff's transformation [11], [13] as

$$\theta(x) = T_l + \frac{1}{\kappa_l}\int_{T_l}^{T} \kappa(T)dT \tag{3}$$

where κ_l is the thermal conductivity of the SWCNT at lower temperatures, which is usually termed as the sink point. The temperature-dependent κ in the absence of mass difference scattering, i.e., for a pure SWCNT, as a result of boundary and second-order three-phonon Umklapp scatterings beyond room temperature, can be written as [2]

$$\kappa(T) = \frac{1}{3E}\left(\frac{k_B}{2\pi^2 v_g}\right)\left(\frac{k_B\Theta_D}{\hbar}\right)^3\left(\frac{v_g}{EL} + T^2\right)^{-1} \tag{4}$$

where k_B is the Boltzmann's constant; $v_g = 10^4$ ms^{-1} is the phonon group velocity; $\Theta_D = 1000$ K is the Debye temperature; $\hbar = h/2\pi$, h is the Planck's constant; and $E = (32/27)\gamma^4(k_B/Mv_g^2)^2\omega_B$ in which parameters $\gamma = 1.24$, $\omega_B =$ 28 GHz, and M are the Gruneisen parameter, phonon branch frequency at the zone boundary, and mass of the carbon atoms, respectively [2].

Using (3) and (4), one can get an approximate linear relationship between θ and T as

$$\theta(x) = T_l + \frac{a}{E\kappa_l b}(T - T_l) \tag{5}$$

where $a = 1/3(k_B/2\pi^2 v_g)(k_B\Theta_D/\hbar)^3$, and $b = v_g/EL$.

Using (5), (1) can be transformed into a linear differential equation as

$$\nabla^2\theta - \alpha_1^2\theta = \beta_1 \tag{6}$$

in which $\alpha_1^2 = \alpha^2 Eb/a$, $\alpha^2 = g/A$, $\beta_1 = (\beta/\kappa_l - \alpha^2 EbT_l/a + \alpha^2 T_l/\kappa_l)$, and $\beta = -(p + gT'/A)$. Using the boundary condition $\theta(-L/2) = \theta_l$ and $\theta(L/2) = \theta_h$, the solution to (6) can be written as

$$\theta(x) = c_1 e^{\alpha_1 x} + c_2 e^{-\alpha_1 x} - \frac{\beta_1}{\alpha_1^2} \tag{7}$$

where

$$\begin{aligned} c_1 = {} & \left[\left(\theta_h + \theta_l + 2\beta_1/\alpha_1^2\right)\sinh(\alpha_1 L/2)\right. \\ & \left.+(\theta_h - \theta_l)\times\cosh(\alpha_1 L/2)\right] \\ & \times\left[4\sinh(\alpha_1 L/2)\cosh(\alpha_1 L/2)\right]^{-1} \end{aligned} \tag{8}$$

$$\begin{aligned} c_2 = {} & \left[\left(\theta_h + \theta_l + 2\beta_1/\alpha_1^2\right)\sinh(\alpha_1 L/2)\right. \\ & \left.-(\theta_h - \theta_l)\times\cosh(\alpha_1 L/2)\right] \\ & \times\left[4\sinh(\alpha_1 L/2)\cosh(\alpha_1 L/2)\right]^{-1} \end{aligned} \tag{9}$$

in which, using (5), we get $\theta_l = T_l$ and $\theta_h = T_l + a(T_h - T_l)/Eb\kappa_l$.

Thus, from (5), the actual temperature T can be written as

$$T(x) = T_l + \frac{E\kappa_l b}{a}\left(\theta(x) - T_l\right). \tag{10}$$

At this point, it should be noted that, in our model, we have considered electrical contact resistance R_c at the interconnects strictly to be an isothermal one, which, in general, is not, and rather becomes surface energy balances. However, in a realistic case, R_c depends on the type of metal. For instance, it would be relatively low if the contacts were made up of Pt, Pd,

etc. In such cases, these effects will not perturb much to the temperature profile along the length of the SWCNT.

In the presence of mass difference scattering, κ can approximately be written as [2]

$$\kappa = \frac{\eta}{\xi}\left(ET^2 + \frac{v_g}{L}\right)^{-1} \tag{11}$$

where $\eta = k_B/2\pi^2 v_g (k_B/\hbar)^3$; $\xi = 15\sqrt{2}/\pi^4 (k_B/\hbar)^3 (V_0 \Gamma_m L/4\pi v_g^4)$, in which $V_0 (= h_t R_0^2)$ is the volume per atom; $h_t = 0.335$ nm and $R_0 = 0.14$ nm [2] are the effective wall thickness and in-plane interatomic distance, respectively; and Γ_m is the form factor of the mass difference scattering. It should be noted that the electrical resistance of an SWCNT generally arises due to different forms of scattering phenomena between electrons and phonons. However, in case of an impure SWCNT, the electrical resistance is independent of the mass difference scattering, which arises due to the difference in atomic mass of the carbon atoms.

Using (3) and (11), the approximate linear relationship between θ and T for the present case can be written as

$$\theta(x) = T_l + \frac{\eta}{\xi \kappa_l E T_l^2}\left(T(x) - T_l\right) \tag{12}$$

where the boundary conditions for θ are $\theta_l = T_l$, and $\theta_h = T_l + \eta/\xi\kappa_l E T_l^2 (T_h - T_l)$. The use of (3) and (12) in (1) results in a similar linear differential equation

$$\nabla^2\theta - \alpha_2^2\theta = \beta_2 \tag{13}$$

in which $\alpha_2^2 = \alpha^2 \xi E T_l^2/\eta$ and $\beta_2 = \beta/\kappa_l + \alpha^2 T_l/\kappa_l - \alpha^2 \xi E T_l^3/\eta$. Using the boundary condition $\theta(-L/2) = \theta_l$ and $\theta(L/2) = \theta_h$, the solution to (13) can be written as

$$\theta(x) = c_3 e^{\alpha_2 x} + c_4 e^{-\alpha_2 x} - \frac{\beta_2}{\alpha_2^2} \tag{14}$$

where

$$\begin{aligned} c_3 = {} & \left[\left(\theta_h + \theta_l + 2\beta_2/\alpha_2^2\right)\sinh(\alpha_2 L/2) + (\theta_h - \theta_l)\right. \\ & \left.\times \cosh(\alpha_2 L/2)\right] \\ & \times \left[4\sinh(\alpha_2 L/2)\cosh(\alpha_2 L/2)\right]^{-1} \end{aligned} \tag{15}$$

$$\begin{aligned} c_4 = {} & \left[\left(\theta_h + \theta_l + 2\beta_2/\alpha_2^2\right)\sinh(\alpha_2 L/2)\right. \\ & \left.-(\theta_h - \theta_l) \times \cosh(\alpha_2 L/2)\right] \\ & \times \left[4\sinh(\alpha_2 L/2)\cosh(\alpha_2 L/2)\right]^{-1}. \end{aligned} \tag{16}$$

Thus, using (12), the actual temperature can be written as

$$T(x) = T_l + \frac{\xi \kappa_l E T_l^2}{\eta}\left(\theta(x) - T_l\right). \tag{17}$$

Equations (10) and (17) specify the temperature profiles along the length of the SWCNT, whose extreme ends are at different temperatures for pure and impure conditions, respectively. The point where the temperature is maximum, which is also known as the hot-spot location, along the length of the SWCNT for both pure and impure cases, can be found by differentiating (10) and (17) with respect to x and equating it to zero. This can be written as

$$x_{\text{pure}} = \left(\frac{1}{2\alpha_1}\right) ln \left|\frac{c_2}{c_1}\right| \tag{18}$$

$$x_{\text{impure}} = \left(\frac{1}{2\alpha_2}\right) ln \left|\frac{c_4}{c_3}\right| \tag{19}$$

respectively.

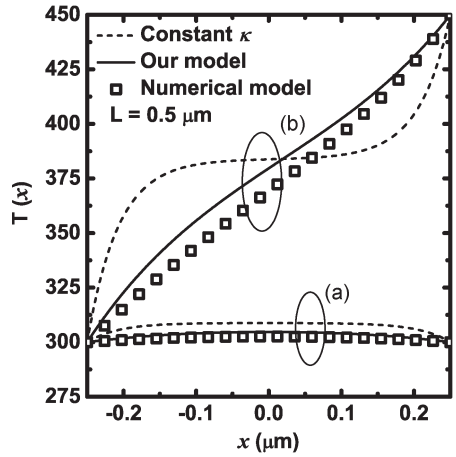

Fig. 2. T as function of x for pure metallic SWCNT for constant κ, our analytical model and numerical model using $I = 5$ μA. (a) represents the three models, with same temperature at the two ends of the tube. (b) represents all the aforementioned models with one end at 300 K and other end is at 450 K.

III. Results and Discussions

Using the aforementioned spectrum constants for metallic SWCNTs, a consistent result is exhibited by the present analytical model, as shown in Fig. 2, for a length of 0.5 μm. We have compared our analytical model (10) with that of the numerical solution of (1) using (4) and with the analytical solution of the Joule-heating equation for pure SWCNT having constant κ, respectively. The temperature profile along the length of a pure SWCNT has been plotted when both ends are at the same temperature of 300 K and when one end is at 300 K and the other is at 450 K, as shown in groups (a) and (b), respectively, in Fig. 2. It is seen that there is less than 2% error between our analytical model and the numerical solution. In the case of constant κ, significant deviation is observed near both ends of the tube when at different temperatures. The plot of the analytical and numerical results at lower currents such as 5 μA appears to be more linear than that compared with constant κ. However, near the midpoint of the tube, they tend to have the same value. It should be noted that, for a tube length of 0.5 μm, sink temperature thermal conductivity has been taken to be 148 $\text{Wm}^{-1}\text{K}^{-1}$. Since it is known that an increase in the tube length increases κ [2], it results in a more flattened nature of the curve for the solution using a constant κ near the mid-zone compared with our analytical and numerical solutions. In case of 1-μm-long SWCNT and a very high current, e.g., 40 μA, a complete nonlinear variation in the temperature profile throughout the length is seen, as shown in Fig. 3. The sink temperature thermal conductivity for such a case has been taken to be 2000 $\text{Wm}^{-1}\text{K}^{-1}$. It appears that, when both ends are at

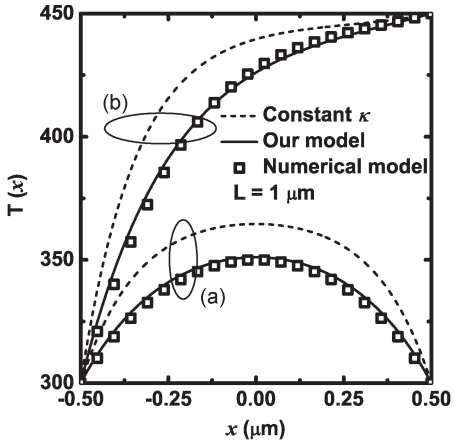

Fig. 3. T as a function of x for all cases of Fig. 2 using $I = 40\ \mu$A.

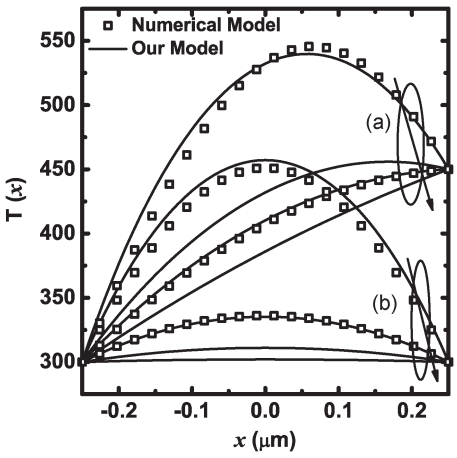

Fig. 4. T as a function of x for impure metallic SWCNT for our analytical and numerical model using $L = 0.5\ \mu$m and $I = 40\ \mu$A when the two ends of the tube are at (a) different temperatures of 300 and 450 K and (b) the same temperature of 300 K. The arrow points the variation of Γ_m, starting from 5×10^{-3} in alternate decreasing steps of 1 and 5×10^{-1}, respectively.

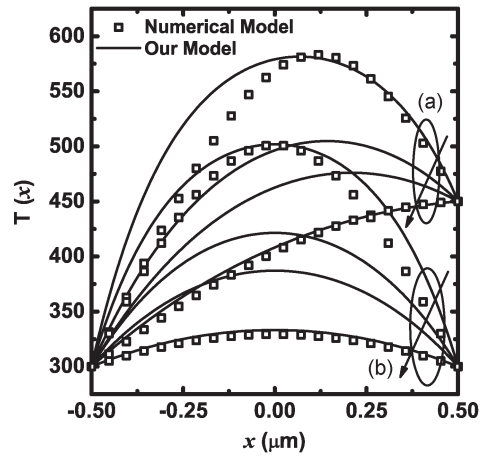

Fig. 5. T as a function of x for impure metallic SWCNT for our analytical and numerical models using $L = 1\ \mu$m and $I = 40\ \mu$A for all the cases of Fig. 4.

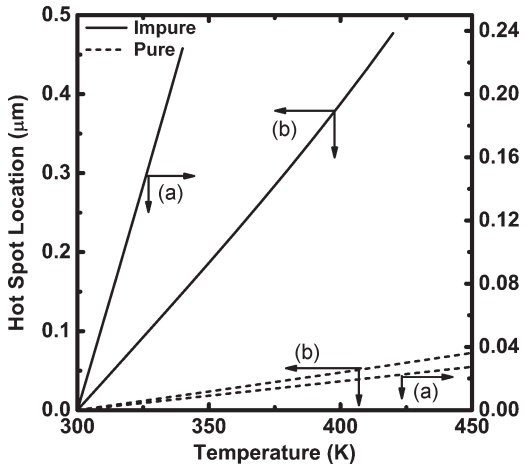

Fig. 6. Hot-spot location along the length of impure ($\Gamma_m = 10^{-4}$) and pure SWCNT as a function of T, whose one end is at 300 K, whereas the temperature at the other end varies for different tube lengths of (a) 0.5 and (b) 1 μm.

room temperature, a temperature difference of about 15 K is exhibited.

The dependence of the temperature profile on the form factor is exhibited in Figs. 4 and 5 for SWCNT lengths of 0.5 and 1 μm, respectively. In Fig. 4, we see that the use of the solution for a pure SWCNT marks a significant difference, compared with our analytical and numerical solutions for the impure SWCNT. With the decrease in the magnitude of the form factor or, in other words, the increase in the purity of the SWCNT, the temperature rise also decreases. This is highly expected in this case since a decrease in Γ_m indicates lesser scattering due to the mass difference effect. This lowering of the mass difference scattering increases sharply the thermal conductivity of the SWCNT, which further lowers down the overall rise in temperature. As Γ_m decreases, all the curves in Fig. 4 for all the solutions tend to merge with their corresponding saturation value of the pure SWCNT under identical conditions. In addition, due to the temperature dependence of the thermal conductivity in an impure SWCNT, there is a significant deviation in $T(x)$ between our analytical model and the solution of constant κ for corresponding variation of Γ_m. Using the analytical model, a temperature rise of about 400 K near the middle of the SWCNT is exhibited with a form factor of 1×10^{-6} and a current of 40 μA. However, it can be found that, for the solution of constant κ, the temperature rise may also overshoot to approximately double the former value. We also see an approximately linear variation of $T(x)$ along the length, which is radically different from the curve of constant κ, as presented in Fig. 2. In Fig. 5, we have shown the variation of $T(x)$ for different values of Γ_m, starting from 5×10^{-3} in alternate decreasing steps of 1 and 5×10^{-1}, respectively, for both the aforementioned temperature conditions.

In Fig. 6, using (18) and (19), we have plotted the location of hot spots along the length of the SWCNT as functions of temperature with the analytical model for both pure and impure tubes having lengths of 0.5 and 1 μm, respectively. Striking differences are exhibited when compared to the curves in Fig. 6 for both pure and impure SWCNT. For a particular SWCNT length, in the presence of mass difference scattering, a wide separation is observed. It appears that, for a 1-μm tube length and a current of 40 μA, the hot-spot location can reach up to 0.98 μm from the sink point contact for an impure SWCNT with $\Gamma_m = 10^{-4}$ between room temperature and 420 K. However, for a 0.5-μm SWCNT with the same level of impurity, the hot-spot location

is about 0.48 μm from the sink point contact. It should be noted that the hot-spot location appears only when both c_1 and c_2 for pure SWCNT and c_3 and c_4 for impure SWCNT are of the same sign for definite values of source and sink point temperature and current levels.

In each of Fig. 2–6, the thermal conductivity for every case has been evaluated by considering the corresponding Γ_m. Approximations have been laid down to make the relation between θ and T linear in order to generate a closed-form solution of (3). This leads to a maximum error between our analytical model and the numerical solution within 5%. This mismatch between the analytical and numerical solutions is due to the fact that the higher order terms appearing in (3) have been neglected because of the involved expression of κ on T in both limits T and T_l. It should be noted that both (6) and (13) have been obtained by linearizing the relation between θ and T in (5) and (12), respectively. Without these approximations, it would not be possible to obtain closed-form solutions for the actual temperature $T(x)$ for both pure and impure SWCNTs. For an impure SWCNT case, approximations have been adopted in (12) using (11) in (3) for limits T and T_l. We have assumed that, for a pure SWCNT within the temperature regime of 300–450 K, $(\theta - T_l)/a\sqrt{b}E\kappa_l \approx 0$ and $T_l(\theta - T_l)/aE\kappa_l \ll 1$, which lead to (10). For the impure SWCNT, the approximation that makes the relation between θ and T a linear one is $\xi\kappa ET_l/\eta(\theta - T_l) < 1$. This approximation can generally be accepted for a current range below 80 μA and $\Gamma_m \leq 10^{-3}$. At this point, it is to be noted that an accurate electrothermal modeling demands an exact solution of the Joule-heating equation (1), where a proper definition of the heat loss to the substrate per unit length for different lengths of SWCNT under different physical conditions and resistance as function of temperature is needed. In this paper, we have neglected these issues and have considered $g = 0.17$ $\mathrm{Wm^{-1}K^{-1}}$ [12] and $R - R_c = 30$ kΩ, where R is the electrical resistance of the SWCNT and the value of R_c depends on the type of metal contact with SWCNT. However, there is no loss of generality in defining temperature-independent resistance approximation in this work since, below a length of 2 μm, the mean-free path of electrons in the metallic SWCNT are weakly dependent on temperature. In addition, the variation of g can be treated to be a geometrical issue and may be asserted as a user-defined parameter. In case of SWCNT via lengths > 2 μm, one has to specifically solve (1) by considering a temperature-dependent resistance model.

We wish to state that the present formulation is based on the derivation of diffusive longitudinal lattice thermal conductivity. It is well known that the thermal conductivity of SWCNT is anisotropic, where the transverse conduction differs widely and is, presumably, orders of magnitude lower than the longitudinal conduction due to extremely high aspect ratio [16]. Although the longitudinal thermal analysis of an individual metallic SWCNT on oxide has been recently reported [12], the heat transport mechanism in their bundles as interconnects by considering the thermal crosstalk along the transverse direction is not fully understood yet. At this stage, the analysis of the temperature profile by considering the lateral thermal conductivity is beyond the scope of this study. The methodologies assigned in this work can be useful for an accurate analysis of temperature profile along the CNT-based interconnects, where the thermal conductivity is mainly determined by its diffusive part.

IV. Conclusion

Using a temperature-dependent thermal conductivity model, this paper has addressed a closed-form analytical solution of the Joule-heating equation in metallic SWCNTs. The effect of mass difference scattering has also been introduced for a complete electrothermal analysis of impure SWCNTs. It has been found that an increase in the form factor of the mass difference scattering severely increases the temperature rise along the length of the SWCNT. In addition, we have compared our analytical results with the corresponding numerical solutions and the solutions for constant thermal conductivity. For all the cases, our analytical model agrees well with the numerical solution.

References

[1] E. Pop, D. Mann, Q. Wang, K. Goodson, and H. Dai, "Thermal conductance of an individual single-wall carbon nanotube above room temperature," *Nano Lett.*, vol. 6, no. 1, pp. 96–100, Jan. 2006.

[2] S. Bhattacharya, R. Almaraj, and S. Mahapatra, "Physics-based thermal conductivity model for metallic single-walled carbon nanotube interconnects," *IEEE Electron Device Lett.*, vol. 32, no. 2, pp. 203–205, Feb. 2011.

[3] Z. L. Wang, D. W. Tang, X. H. Zheng, W. G. Zhang, and Y. T. Zhu, "Length-dependent thermal conductivity of single-wall carbon nanotubes: Prediction and measurements," *Nanotechnology*, vol. 18, no. 47, p. 475 714, Nov. 2007.

[4] T. Gupta, *Copper Interconnect Technology*. New York: Springer-Verlag, 2009.

[5] N. Srivastava, H. Li, F. Kreupl, and K. Banerjee, "On the applicability of single-walled carbon nanotubes as VLSI interconnects," *IEEE Trans. Nanotechnol.*, vol. 8, no. 4, pp. 542–559, Jul. 2009.

[6] A. Naeemi and J. D. Meindl, "Design and performance modeling for single-walled carbon nanotubes as local, semiglobal, and global interconnects in gigascale integrated systems," *IEEE Trans. Electron Devices*, vol. 54, no. 1, pp. 26–37, Jan. 2007.

[7] A. Nieuwoudt and Y. Massoud, "On the optimal design, performance, and reliability of future carbon nanotube-based interconnect solutions," *IEEE Trans. Electron Devices*, vol. 55, no. 8, pp. 2097–2010, Aug. 2008.

[8] W. C. Chen, W.-Y. Yin, L. Jia, and Q. H. Liu, "Electrothermal characterization of single-walled carbon nanotube (SWCNT) interconnect arrays," *IEEE Trans. Nanotechnol.*, vol. 8, no. 6, pp. 718–728, Nov. 2009.

[9] A. Hosseini and V. Shabro, "Thermally-aware modeling and performance evaluation for single-walled carbon nanotube-based interconnects for future high performance integrated circuits," *Microelectron. Eng.*, vol. 87, no. 10, pp. 1955–1962, Oct. 2010.

[10] K. Sun, M. A. Stroscio, and M. Dutta, "Thermal conductivity of carbon nanotubes," *J. Appl. Phys.*, vol. 105, no. 7, pp. 074316 (1)–074316 (5), Apr. 2009.

[11] H. S. Carslaw and J. C. Jaeger, *Conduction of Heat in Solids*. Oxford, U.K.: Oxford Univ. Press, 1959.

[12] E. Pop, D. A. Mann, K. E. Goodson, and H. Dai, "Electrical and thermal transport in metallic single-wall carbon nanotubes on insulating substrates," *J. Appl. Phys.*, vol. 101, no. 9, pp. 093710 (1)–093710 (9), May 2007.

[13] W. B. Joyce, "Thermal resistance of heat sinks with temperature dependent conductivity," *Solid-State Electron.*, vol. 18, no. 4, pp. 321–322, Apr. 1975.

[14] F. P. Incropera, D. P. DeWitt, T. L. Bergman, and A. S. Lavine, *Fundamentals of Heat and Mass Transfer,* 6th ed. New York: Wiley, 2007, pp. 2–168.

[15] S. Bhattacharya and S. Mahapatra, "Simplified theory of carrier backscattering in semiconducting carbon nanotubes: A Kane's model approach," *J. Appl. Phys.*, vol. 107, no. 9, pp. 094314 (1)–094314 (7), May 2010.

[16] [Online]. Available: http://www.itrs.net/Links/2009ITRS/2009Chapters_2009 Tables/2009_-Interconnect.pdf

Rekha Verma received the B.E. degree in electronics and communication engineering from the University of Rajasthan, Jaipur, India, in 2003 and the M.Tech. degree in electrical engineering, with specialization in VLSI design, from Banasthali Vidyapith, Banasthali, India, in 2009. She is currently working towards the Ph.D. degree in electrothermal transport in nanoscale devices and their interconnects at Nano-Scale Device Research Laboratory, Centre for Electronics Design and Technology, Indian Institute of Science, Bangalore, India.

Sitangshu Bhattacharya received the B.S. and M.S. degrees in physics and electronic science from the University of Calcutta, West Bengal, India, in 2001 and 2003, respectively, and the Ph.D. degree in physics and electronic science from Jadavpur University, Calcutta, India, in 2009.

He is currently a Postdoctoral Young Scientist with the Nano-Scale Device Research Laboratory, Centre for Electronics Design and Technology, Indian Institute of Science, Bangalore, India. He coauthored four monographs entitled *Einstein Relation in Compound Semiconductors and Their Nanostructures*, *Photoemission from Optoelectronic Materials and their Nanostructures*, *Thermoelectric Power in Nanostructured Materials Under Strong Magnetic Field*, and *Fowler-Nordheim Field Emission from Semiconductors and their Nanostructures* in the Springer Series in Materials Science, Solid States Science and Nanostructured Science and Technology. He is the author and coauthor of more than 40 journal publications. He is also an invited speaker at different international conferences related to electrothermal transport. His current research interests include theoretical investigation of different diffusive mode electronic and thermal transport properties of low-dimensional structures and devices under external controlled fields using tight binding theory.

Santanu Mahapatra (M'08–SM'10) received the B.E. degree in electronics and telecommunications from Jadavpur University, Kolkata, India, in 1999, the M.Tech. degree in electrical engineering, with specialization in microelectronics, from Indian Institute of Technology, Kanpur, India, in 2001, and the Ph.D. degree in electrical engineering from the Swiss Federal Institute of Technology-Lausanne (EPFL), Lausanne, Switzerland, in 2005. His Ph.D. work was focused on compact modeling of single-electron transistors and their hybridization with complementary metal–oxide–semiconductors (CMOSs).

In August 2005, he was an Assistant Professor with the Center for Electronics Design and Technology (CEDT), Indian Institute of Science, Bangalore, India, where he has been an Associate Professor since September 2010 and was promoted on an out-of-the-term basis. In 2006, he founded the Nano-Scale Device Research Laboratory, CEDT, where his team is currently engaged in research on compact modeling and simulation of emerging nanotechnologies and advanced CMOS devices. He has supervised many students for their M.S. thesis and Ph.D. dissertation. He is the author and coauthor of several papers published in international journals and refereed conference proceedings. He is also the author of the book *Hybrid CMOS Single Electron Transistor Device and Circuit Design* (Artech House, 2006). His current research interests include device reliability, multigate transistors, tunnel field-effect transistors, single-electron transistors, carbon nanoelectronics, and CMOS nanohybridization.

Prof. Mahapatra was the recipient of the Best Paper Award at the International Semiconductor Conference, Romania, in 2003; the IBM Faculty Award in 2007; the Microsoft India Research Outstanding Faculty Award in 2007; and the Associateship of the Indian Academy of Science in 2009.